

## Integrated approach for delineating groundwater potential and quality in District Bagh, Azad Jammu and Kashmir, Pakistan

Abrar Niaz<sup>a,\*</sup>, Usman Basharat<sup>a</sup>, Umair Bin Nisar<sup>b</sup>, Rashida Fiaz<sup>c</sup>,  
Muhammad Saleem Mughal<sup>a</sup>, Fahad Hameed<sup>a</sup>, Aamir Asghar<sup>d</sup>, Jawad Niaz<sup>a</sup>

<sup>a</sup>Institute of Geology, University of Azad Jammu & Kashmir Muzaffarabad, Pakistan, emails: abrar.niaz@ajku.edu.pk (A. Niaz), usmangeology101@gmail.com (U. Basharat), muhammadsaleem152@yahoo.com (M.S. Mughal), fahad.hameed@ajku.edu.pk (F. Hameed), jawadniaz52@gmail.com (J. Niaz)

<sup>b</sup>Centre for Climate Research and Development, COMSATS University Islamabad, Park Road, Tarlai Kalan, 45550 Islamabad, Pakistan, email: umair.nisar@comsats.edu.pk

<sup>c</sup>Department of Chemistry, University of Azad Jammu & Kashmir Muzaffarabad, Pakistan, email: abrarashida@gmail.com

<sup>d</sup>Institute of Geology, University of Poonch, Rawalakot Azad Jammu & Kashmir, Pakistan, email: jojaaamir@gmail.com

Received 7 August 2021; Accepted 1 January 2022

---

### ABSTRACT

The current research integrates vertical electrical sounding (VES) and hydrochemical analysis to delineate water bearing zones, assess their vulnerability to surficial contamination, and implications on water quality of District Bagh, Azad Jammu and Kashmir. In order to achieve the desired results, a total of 45 VES points and 25 water samples were collected from springs, open and bore wells in the study area. The VES data was acquired using ABEM Terrameter SAS 4000. The interpretation of VES data revealed confined to unconfined aquifer systems, furthermore, the aquifer thickness ranges between 5–95 m with the resistivity values of 10–70 Ohm m. Darzarouk parameters were utilized to demarcate the protective capacity of the aquifer system based on a vulnerability map. This map classified the surficial protective capacity from moderate to very good associated with good clay cover that will restrict the surficial infiltration from contaminating the groundwater. The hydrochemical analysis of the area further justified the vulnerability assessment as only 2 samples (9 and 24) out of 24 were found not feasible for drinking. The study will prove useful for the local administration as the population has been drastically increasing in the Bagh District and provision of safe drinking water will be difficult in the future.

*Keywords:* Aquifer vulnerability; Hydrochemical analysis; Vertical electrical sounding; Water quality

---

### 1. Introduction

Water is an important natural resource and plays a major role in everyday life. Water covers more than seventy percent of the earth's exterior however less than three percent of this is freshwater [1,2]. Out of that freshwater volume of water accessible for human use is only 0.01%; the rest is bound in ice or glaciers [3].

With increasing population and urbanization availability of clean drinking water is becoming a commodity. Due to excessive pumping, the subsurface aquifer systems are under stress. It is a need for time to look for new groundwater resources and map the vulnerability of already existing aquifers. Geophysical methods have been long used for the characterization of subsurface anomalies. Different geophysical methods such as gravity, magnetic, and resistivity

---

\* Corresponding author.

have made their mark in mineral, structure, hydrocarbon and groundwater occurrence/distribution. The geoelectrical method is a geophysical technique that is based on conductivity/resistivity contrast used to determine the distribution of the Earth materials in the subsurface. This method is suitable for identifying lithological units and variations within those units as along with groundwater and aquifer studies [4].

The surface geoelectrical methods, especially the vertical electrical sounding (VES) is comparatively inexpensive and gives better results as compared to other geophysical methods for the investigation of groundwater [5,6]. This quantitative evaluation technique is used to locate the exploration sites as well as for the determination of the underlying geology of the area [7–9]. The calculated resistivity is also utilized in the form of Darzarouk parameters that later on classify the overlying layer of the aquifer system based on protective capacity. These calculations determine (vulnerability mapping) the sensitivity of groundwater quality to an imposed contaminant load, often obtained by the intrinsic characteristics of the aquifer [10–13]. With the help of vulnerability mapping, it is possible to identify which areas are more susceptible to contamination [14].

Deterioration in water quality is another growing problem [15]. Groundwater is becoming progressively contaminated because of numerous anthropogenic actions like indiscriminating waste disposal of municipal and industrial wastes, and large scale applications of agricultural chemicals [15,16]. Anthropogenic activities add numerous harmful ingredients to the water which result in extensive water-borne diseases [12]. Deteriorating water quality is a core ecological and health related concern in Pakistan. Poor living circumstances and natural disasters combined with mismanagement commonly pollute drinking water in Pakistan. Government statistics reveal that 56% of Pakistan's total population has access to safe drinking water but in village regions, clean drinking water is scarcely accessible to 44% of the population. Therefore it is important to examine the pollution of water and its effects on human health and the surrounding environment in Pakistan. In order to classify the water availability and contamination on large scale GIS mapping is used in most parts of the world [13].

GIS has been used in the map classification of groundwater quality, based on correlating total dissolved solids (TDS) values with some aquifer characteristics [13] or land use and land cover [14]. Other studies have used GIS as a database system in order to prepare maps of water quality according to concentration values of different chemical constituents [16–18]

The study area lacks a major river, due to topographical constraints and scattered population surface water is not accessible in most parts of the district. With ever growing population and industrialization, the surface water is not enough for the local community resulting in increased demand for groundwater. In addition to that different factories in the area have also been introducing harmful chemicals in the groundwater system, putting the life of locals at stake. The present study aims to determine the groundwater potential, to carry out aquifer vulnerability assessment, and hydrochemical analysis of different collected samples in the area. This is achieved by integrating

the VES and hydrochemical data sets. The VES data identified the subsurface water bearing zones and classified the overburden layers in terms of aquifer vulnerability. Hydrochemical analysis integrated with GIS mapping provided spatial distribution of water quality in the Bagh District of Azad Jammu & Kashmir Pakistan. The study will be helpful for the local administration in the provision of safe drinking water.

### 1.1. Study area

The study area lies in the Kashmir basin. The area is bounded from 73° 47' 30.48"E to 73° 79' 18"E and from 33° 58' 24.6"N to 33° 97' 35"N (Fig. 1). The area is bordered by the Muzaffarabad (capital) in the North, Poonch in the South, Rawalpindi (Punjab) and Abbottabad (KPK) in the west. The whole area of the Bagh District is 770 km<sup>2</sup> approximately. The majority of the area of District Bagh is mountainous, usually sloping from northeast to southwest. In particular, the mountains are dominated by coniferous and pine forests. The area's altitude ranges between 1,676 and 2,500 m. The summer and winter temperatures are 22°C–35°C and –5°C–13°C, respectively. The average annual precipitation of the area is 1,500 mm. The weather in the area varies from tropical to temperate. Furthermore, this area was severely affected by the October 8, 2005, Kashmir earthquake.

### 1.2. Geology of the study area

The Bagh region is situated in northeast Pakistan's Himalayan mountain belt. The study area is composed of sedimentary rocks because of the Himalayan collision rocks are folded, faulted, fractured and jointed [19]. Table 1 shows the stratigraphic order of the exposed formations in the project area.

## 2. Materials and methods

The research was established on two different parameters a geophysical survey (electrical survey) and physiochemical analysis. The field was deliberate to conduct the geophysical (electrical resistivity) survey of the research area. The 45 stations were selected to perform the electrical (VES) survey using the Schlumberger configuration. Samples of water were collected from different locations. The flow chart for the methodology adopted for the study is shown in the figure below.

### 2.1. Geoelectrical data acquisition and processing

There are several methods in practice for the assessment of hydrogeological conditions, and among these, the geoelectrical resistivity techniques are effective, reliable and feasible [20–22]. At all locations data was acquired by employing the Schlumberger electrode configuration [Eq. (1)] [22]. The acquired data consist of AB/2 values and apparent resistivity.

$$R = \frac{\rho \left[ (AB/2)^2 - (MN/2)^2 \right] \Delta V}{MN I} \quad (1)$$

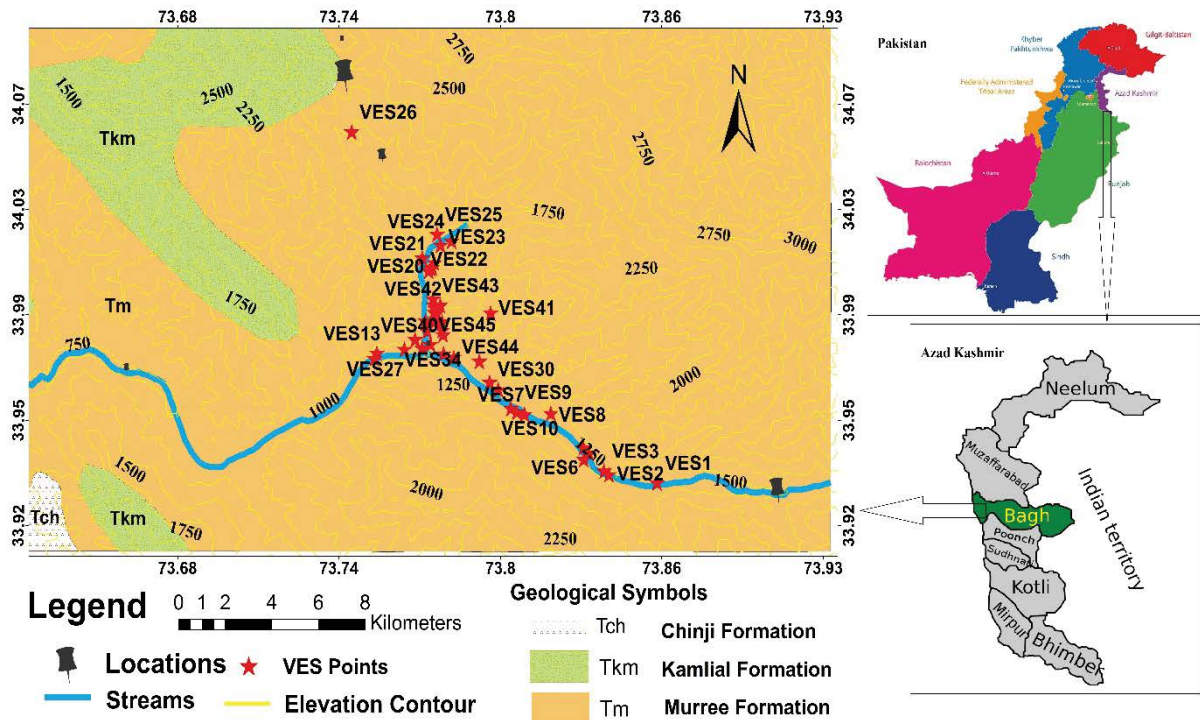


Fig. 1. Location map of the study area.

Table 1  
The stratigraphic order of the formations exposed in the project area

Formation	Age	Lithology
Recent Alluvium	Quaternary	Unconsolidated deposits of sand, clay, and silt with large particles of gravels and boulders.
Chinji Formation	Late Miocene	Greenish grey to light grey, massive medium to coarse-grained sandstone, siltstone, and mudstone. The sandstone alternate with clays. It includes 40% clays and 60% sandstone.
Kamlial Formation	Miocene	Purple grey and dark red sandstone, siltstone and contain intercedes of hard purple shales with intraformational conglomerates.
Murree Formation	Miocene	Cyclic deposits of sandstone, shales, siltstone, and claystone.

where  $AB/2$  is the current electrode spacing,  $MN/2$  is the potential electrode distance,  $V$  is the voltage and  $I$  is the induced current.

The maximum electrode spacing at various locations ranges from 100 to 150 m. The geometric factor “K.” is automatically calculated by the system and presents the ending results as an apparent resistivity on display. Data processing was done after acquirement/acquisition. The field data is processed for the delineation of true resistivity values and depth of subsurface layers. Thus, lithological interpretations of subsurface units have been carried out on the basis of standardized resistivity values. IPI2WIN software was used for the processing of the field data according to the requirements. This software comparatively was easy and appropriate to use. The partial curve matching procedure was used for interpretation after the delineation of curve types. The international technique, auxiliary point diagrams, and two-layer master curves are used. The layer’s thickness and true resistivity of each sounding

station curve was gained. The result of electrical sounding was calculated by the conventional curve matching technique in order to obtain thickness and true resistivity of subsurface rocks layer constituting the different ground models, so IPI2WIN inversion software used these numeric values as a major database. Fig. 1 shows the geology with the location of VES points in the research area.

### 2.2. Sampling

25 samples of water from wells and springs were taken throughout fieldwork in the research area of the Bagh region. Fig. 3 shows the location of the sample. The collected samples were analyzed in the laboratory. The parameters of water quality investigated at each site were: magnesium, calcium, sodium, sulphate ( $SO_4$ ), chloride, bicarbonate ( $HCO_3$ ), nitrate ( $NO_3$ ), pH, electrical conductivity (EC), TDS, and hardness, etc. The fitness of water for domestic use was evaluated by relating the parameter value with the WHO

(World Health Organization) and APHA (American Public Health Association). GIS analysis was performed. IDW (investigated derived waste) computes a value to interpolate the spatial data with the procedure, by multiplying the weighted sum of all the points. The general methodology used for study is presented in Fig. 2.

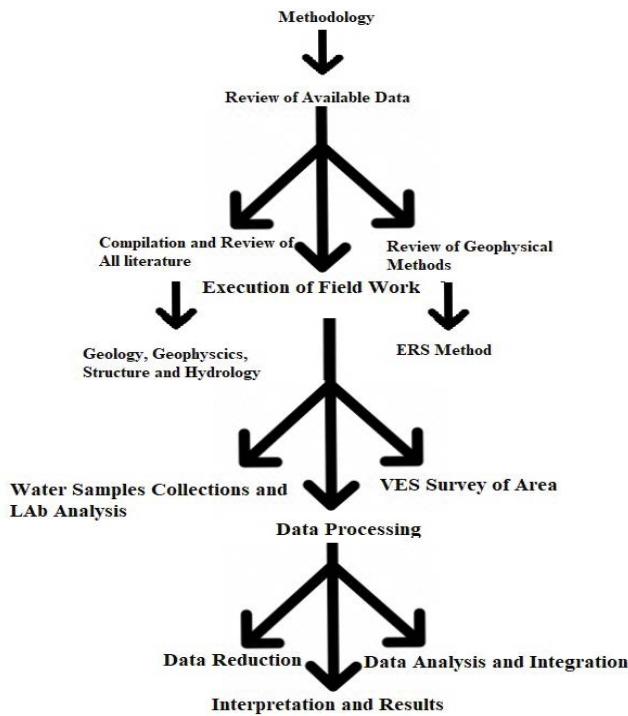


Fig. 2. Methodology adopted for study.

### 3. Results and discussion

The results of resistivity data and physico-chemical analysis have been interpreted quantitatively as well as qualitatively.

#### 3.1. Qualitative interpretation

In qualitative interpretation different apparent resistivity maps of the Bagh area of Azad Jammu & Kashmir have been prepared. Figs. 4–7 illustrate the apparent resistivity maps for different electrode spacing in the study area.

The apparent resistivity is significant for groundwater symptoms through depth. Through iso-resistivity mapping that is possible to demarcate the zone with different groundwater quality [23,24].

In the map for 30 m electrode spacing in the Bagh area (Fig. 4), the contour values vary from 0 to 650 Ohm m. The low values of resistivity in the area are a clear sign of good groundwater potential. The contours of 50–150 Ohm m cover almost the total map except, the southern part of the area where one contours closure with resistivity range 250–350 Ohm m are formed.

In general low values of resistivity varies from 0 to 100 Ohm m for electrode spacing 30 m have been observed in the study area depicting good groundwater potential except in the south-eastern part of the area where resistivity values range from 200–500 Ohm m demarcating moderate potential of groundwater.

In the maps for electrode spacing of 50 and 70 m Figs. 5 and 6, the apparent resistivity ranged from 0 to 190 Ohm m and 0 to 210 Ohm m respectively. The low values of resistivity in the research area are the clear signs and indications of good groundwater potential. The North-west and central

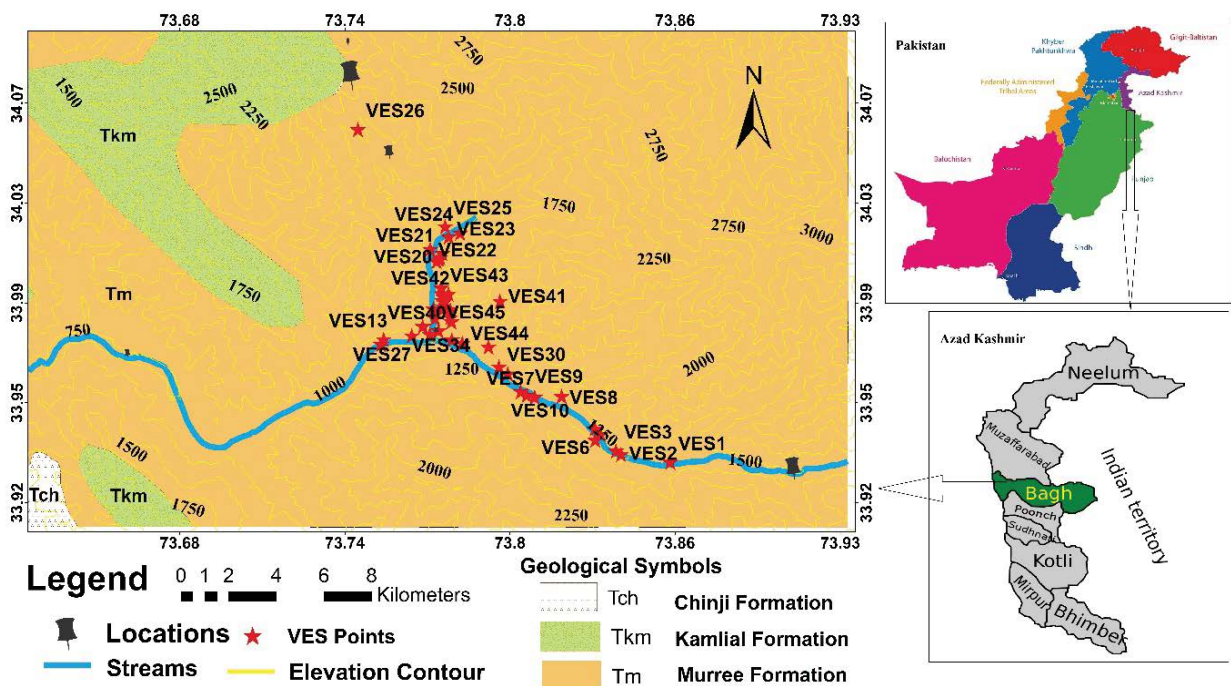


Fig. 3. Showing the location of VES points in the research area.

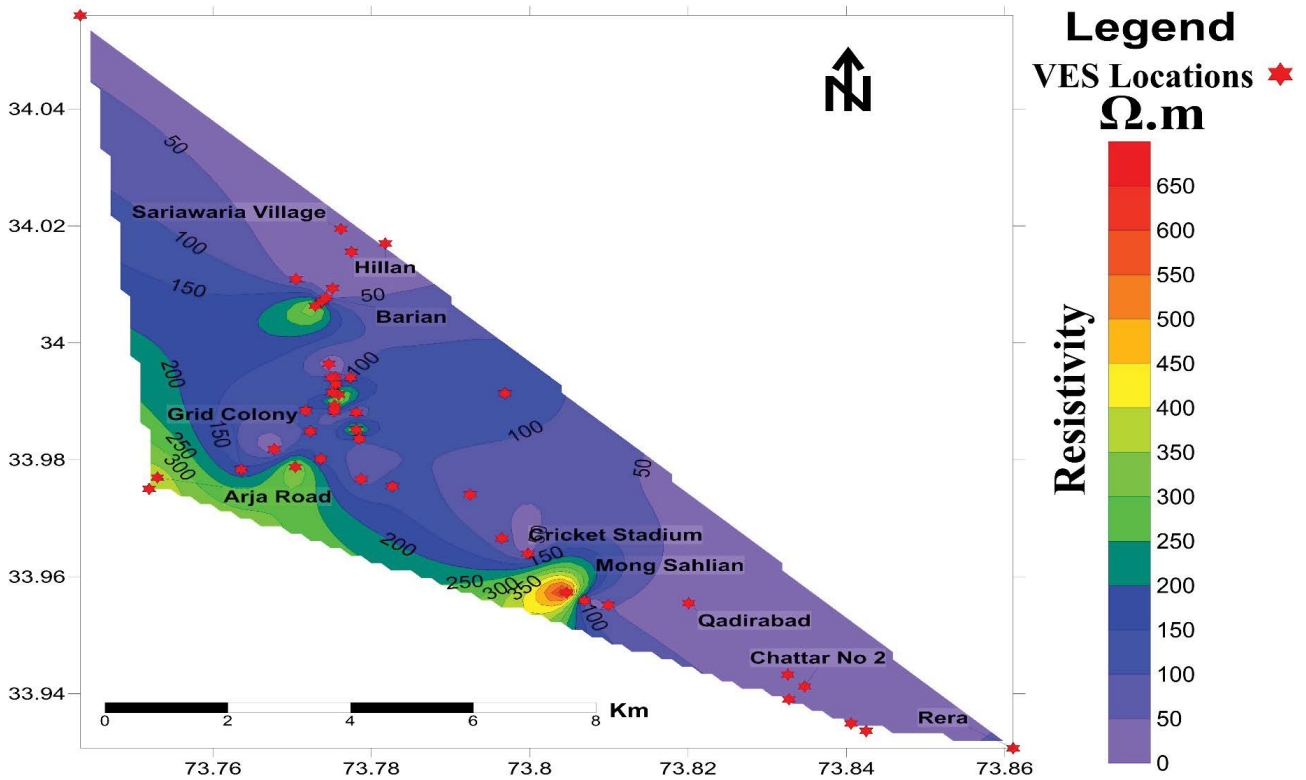


Fig. 4. Apparent resistivity map of Bagh area at 30 m electrode spacing.

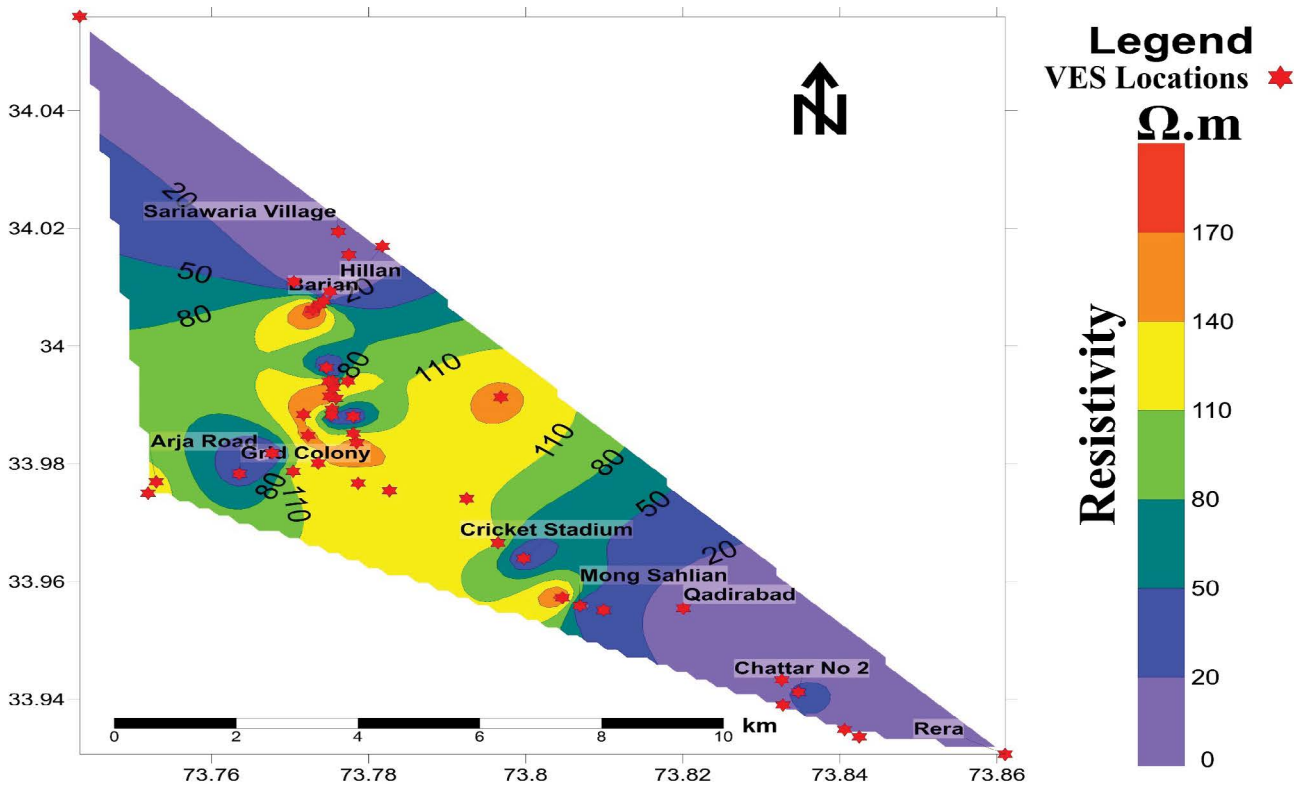


Fig. 5. Apparent resistivity map of Bagh area at 50 m electrode spacing.

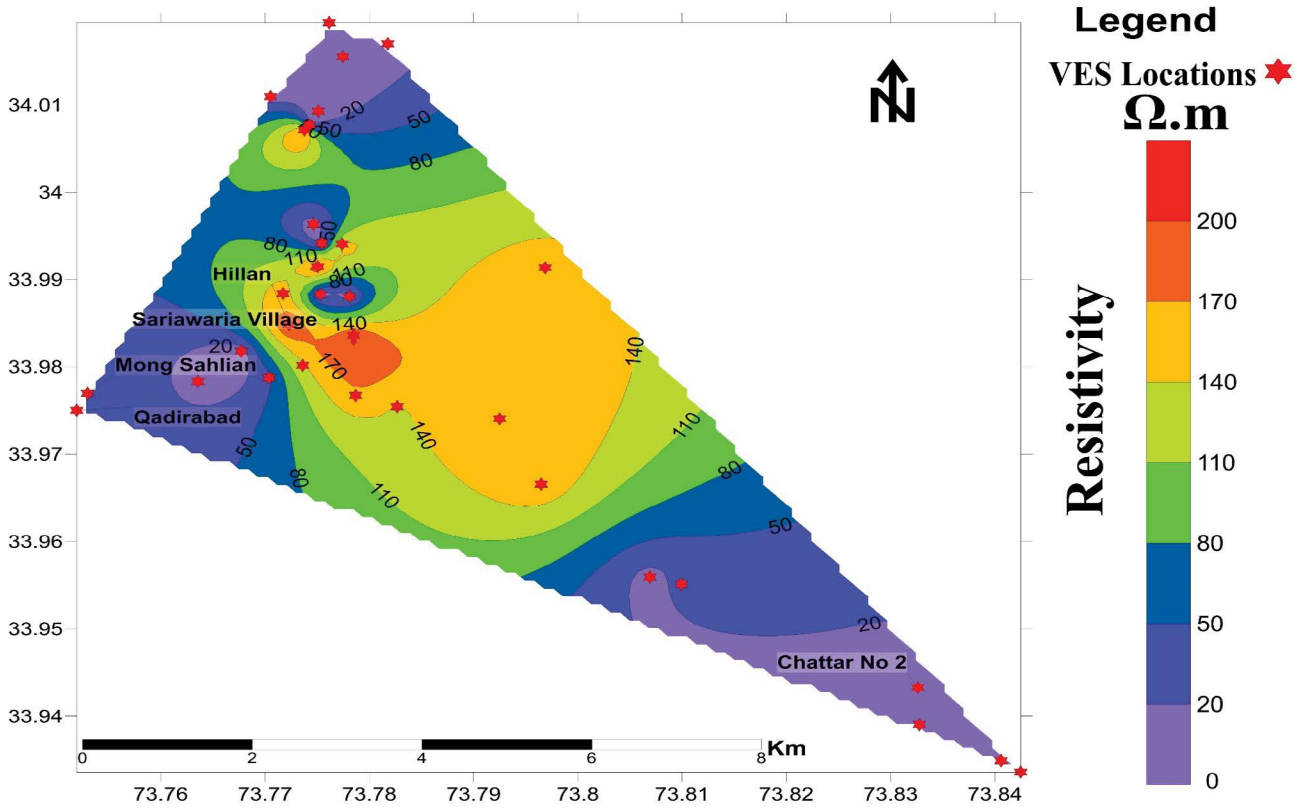


Fig. 6. Apparent resistivity map of Bagh area at 70 m electrode spacing.

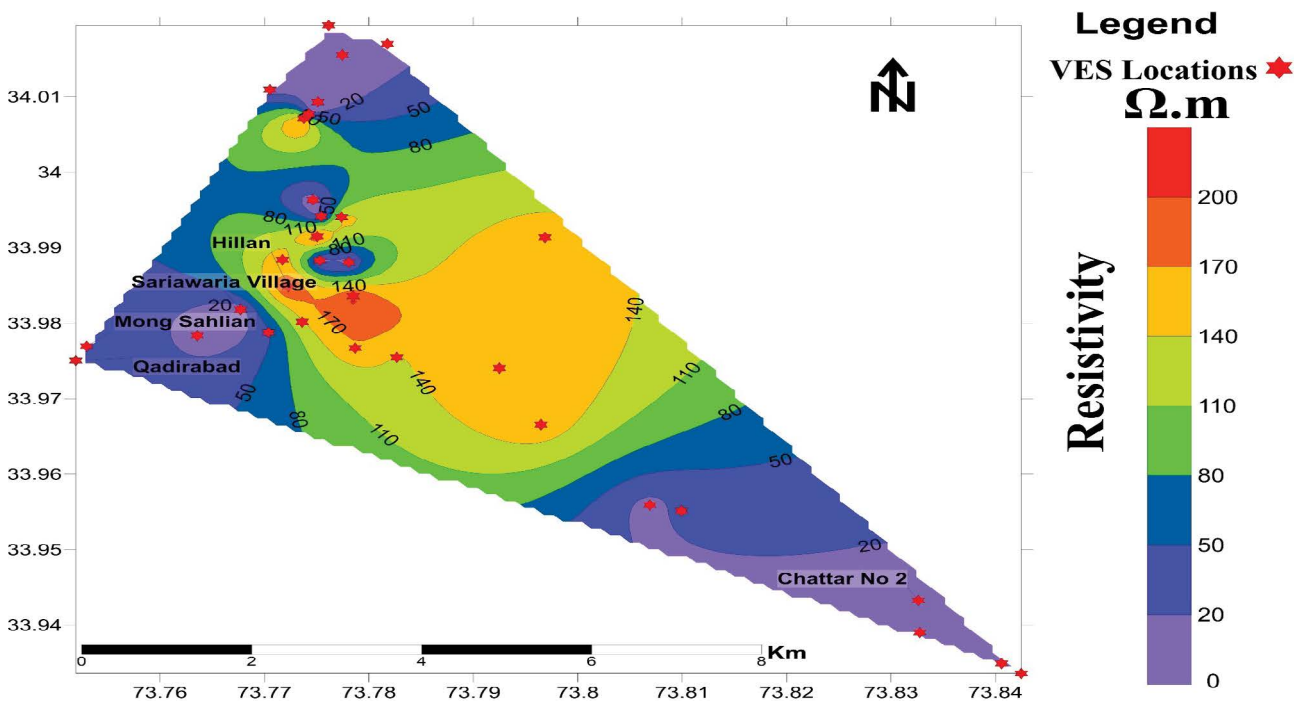


Fig. 7. Apparent resistivity map of Bagh area at 100 m electrode spacing.

portion of the maps are categorized by high values of apparent resistivity and four closures with resistivity ranging from 100 to 150 Ohm m.

The low resistivity values (0–50 Ohm m) in both maps (Figs. 5 and 6) have been observed in the north-west and southeastern part of the study area at electrode spacing 50 m indicating the good potential of groundwater. The central part of the study area at this depth shows relatively moderate to high resistivity (70–200 Ohm m).

In the map for 100 m electrode spacing (Fig. 7), the contour values vary from 10 to 270 Ohm m. North and central part of the area where three contours closures with resistivity range 170 to 270 Ohm m are formed. In Sariawaria village and Hillian area resistivity varies from 0 to 10 Ohm m. Low values indicate signs of groundwater potential. In the Mong Sahlian area, the resistivity varies from 10 to 30 Ohm m for 100 m electrode spacing. Low values of resistivity 10 to 70 Ohm m in the area are a clear sign of good groundwater potential.

3.2. Quantitative interpretation

The quantitative interpretation of 45 VES (vertical electrical sounding) points of the Bagh area of Azad Kashmir has been done. IPI2WIN software, a resistivity modelling system prepared by the University of Moscow Russia was utilized for quantitative interpretation of the resistivity data. IPI2WIN can be used for both forward and inverse modelling modes. To get these suitable initial parameters for use in the IPI2WIN, the sounding resistivity data were passed through the process of the partial curve matching technique. The apparent resistivity values of each VES were plotted along *x*-coordinate on a transparent log-log paper against the half current electrode spacing (AB/2) along *y*-coordinate. In measurement resistivity with Schlumberger configuration, the resistivity graph consists of segments that parallel with the different values of the potential electrode spacing [25,26].

The subsurface lithological models were also developed by using Sed-log software for all 45 profiles based on the true resistivity. The overall depth achieved in the area ranges from 50 to 100 m. Figs. 8–12 show the models of the subsurface lithology of the area. The lithology is dominated by clay matrix, sandy soil, sandy clay, boulder clay, siltstone with variable thickness of sand. The compact sandstone is also existing which indicates high resistivity values.

Fig. 8 shows the litholog of profiles 1–9. In this figure shows subsurface geology comprised of dry sandy soil, clay, boulder clay and sandstone.

Fig. 9 shows subsurface litho-logs of profile 10–18. In this figure, the resistivity values ranging from 1,000 to 1,800 Ohm m are interpreted as sandstone deposits. The low resistivity values in from 30 to 100 Ohm m and 3 to 30 Ohm m, respectively indicate the clays deposits.

Fig. 10 shows the litho-logs of profile 19. In this pseudo-section, the values ranging from 91 to 120 Ohm m are inferred as clay deposits. The low resistivity values range from 4.37 to 10 Ohm m and 0.848 to 7.2 Ohm m respectively indicates clays deposits.

Fig. 11 presents the lithologs of VES 27 to VES 36 indicates the subsurface lithology. In this figure, the resistivity ranging from 251 to 631 Ohm m is interpreted as sandstone deposits. The low resistivity values in blue and green colour range from 2.51 to 39.8 Ohm m and 0.774 to 59.9 Ohm m indicate the clays deposits respectively.

Fig. 12 presents the litho-logs of VES 37 to VES 45 indicates the subsurface lithology. The resistivity ranges from 289 to 838 Ohm m is interpreted as sandstone deposits. The low resistivity values in the range from 1.43 to 100 Ohm m and 0.501 to 200 Ohm m indicate the clays deposits respectively.

3.3. Aquifer thickness map

The map of the aquifer thickness (Fig. 13), could be used in classification geological units because the amount

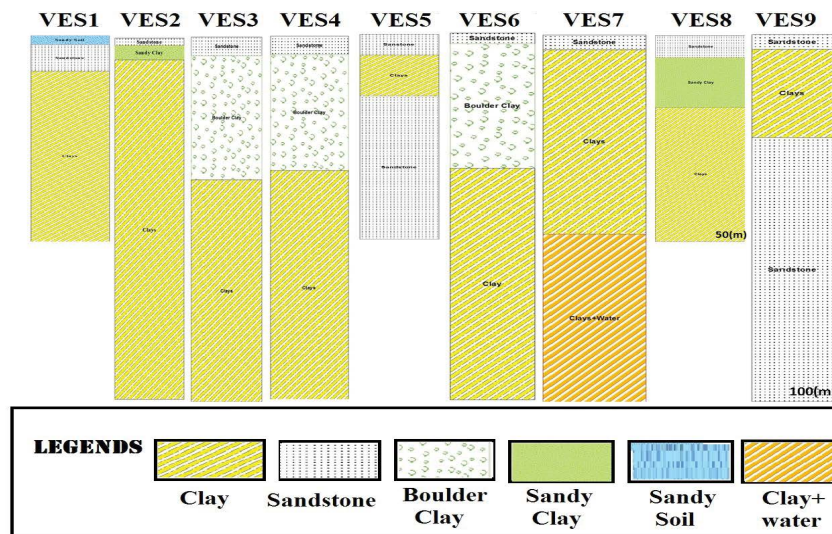


Fig. 8. Lithological model of the Bagh area from VES 1 to VES 9 calculated on the basis of resistivity.

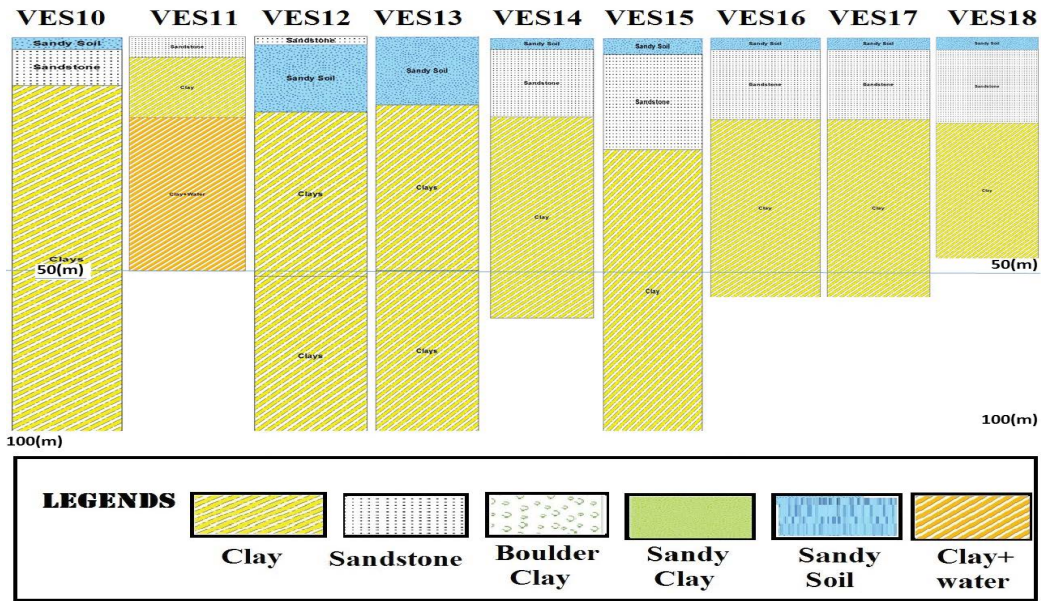


Fig. 9. Lithological model of the Bagh area from VES 10 to VES 18 calculated on the basis of resistivity.

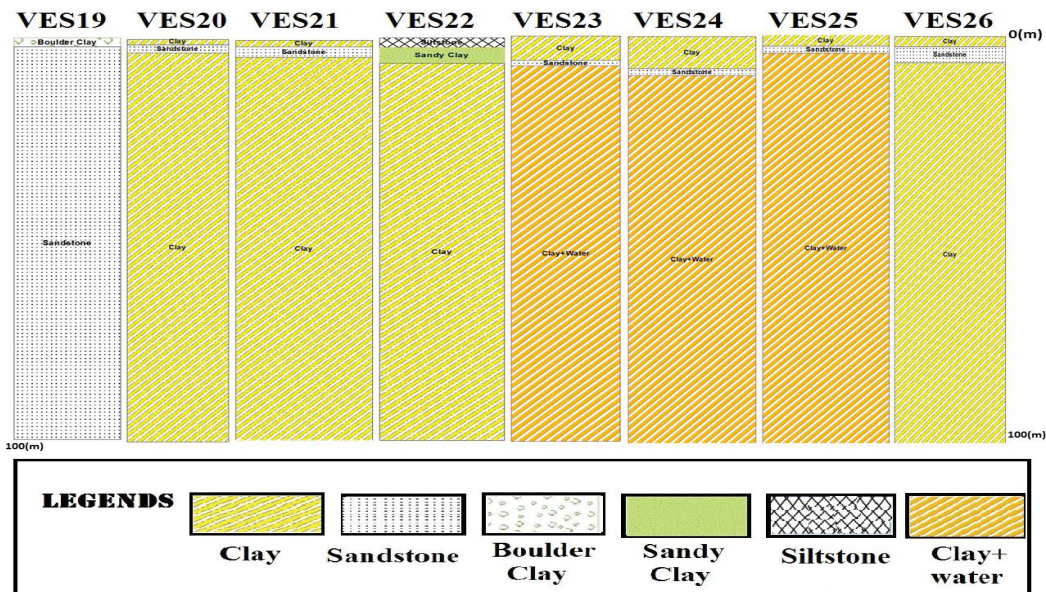


Fig. 10. Lithological model of the Bagh area from VES 19 to VES 26 calculated on the basis of resistivity.

of water from each vertical electrical sounding location depends on the aquifer thickness [27]. The total region could be categorized as a moderate to good groundwater prospective zone. The study discloses that “good” potential exists at the southwestern portion as well as the north-eastern part of the research region with thickness ranges of 0–60 m. “Moderate” groundwater potential zone having an aquifer thickness 60–90 m and delineated in the south-eastern and central portion of the Bagh region.

In the north-western and southern parts of the study area, the aquifer thickness varies from 0 to 20 m which lies in a moderate groundwater potential zone. In the central

part of the study area, the aquifer thickness was calculated 30–55 m depicting good potential of water. In the Barian area, aquifer thickness varies from 5 to 15 m which is also a moderate groundwater potential zone. In the Arja road area the aquifer thickness varies from 5 to 15 m and in the grid station area aquifer thickness varies from 0 to 5 m which exists in a moderate groundwater potential zone. In cricket stadium the aquifer thickness range is 0–5 m which occurs in moderate groundwater potential zones. In the Mong Sahlian area aquifer thickness varies from 30 to 35 m, occurs in moderate groundwater potential zones.

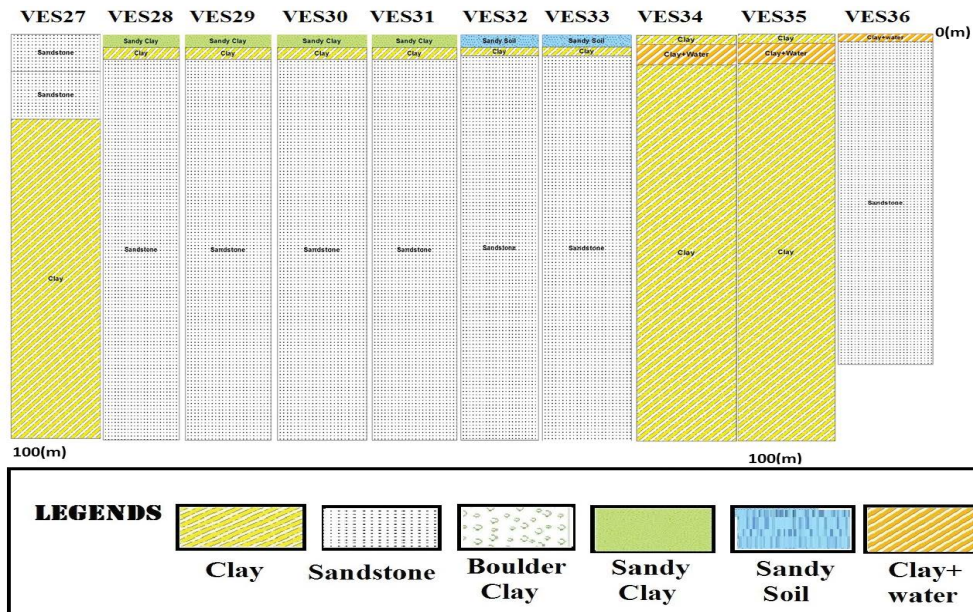


Fig. 11. Lithological model of the Bagh area from VES 27 to VES 36 calculated on the basis of resistivity.

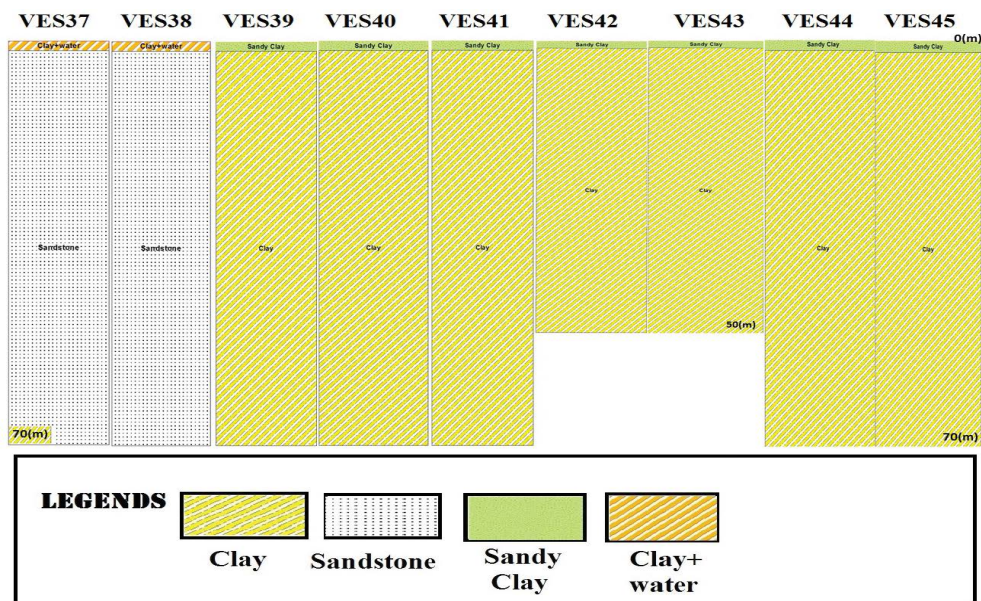


Fig. 12. Lithological model of the Bagh area from VES 37 to VES 45 calculated on the basis of resistivity.

### 3.4. Longitudinal conductance (S)

It is described as conductance through a column of 1 m along the direction of the bedding plane is denoted by “S” and its unit is siemens/m [28–31].

$$S = \frac{h_1}{\rho_1} = \frac{h_2}{\rho_2} \quad (2)$$

$$S = \frac{h}{\rho}$$

where “ρ” is resistivity and “h” is layer thickness. High “S” usually shows comparatively dense succession and would be rendered great significance in terms of groundwater perspective and vice versa. The flowing current is measured by the Law of Ohm while the flow of groundwater is directed by the Law of Darcy and the relation between hydraulic and electric parameters is generally established [32–36]. Protective capacity grading is given in Table 2.

The research area’s vulnerability map was prepared by unit longitudinal conductance. Fig. 14 shows the distribution pattern of the overload protective capacity of aquifers in the research area. The above grading helped

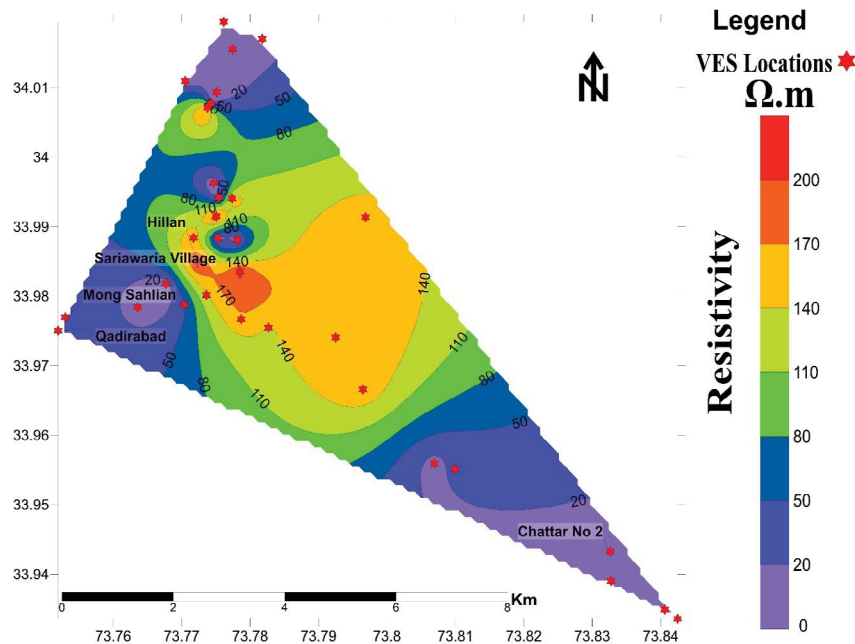


Fig. 13. Aquifer thickness map of the Bagh area.

Table 2  
Rating of protection capacity [34]

Longitudinal conductance (mhos)	Protective capacity rating
>10	Excellent
5–10	Very Good
0.7–4.9	Good
0.2–0.69	Moderate
0.1–0.19	Weak
<0.1	Poor

in the categorization of the project zone into “modest”, “good”, “very good” protection capacity regions. Areas classified into “good”, “very good” and “excellent” are less susceptible or vulnerable to contamination [37,38]. The study area map generally shows that the aquifer overburden protection capacity is “Excellent” in the north-western zone of the research area. The longitudinal conductance values of 0–19 mhos.

The above-cited rating is very helpful for grouping of the project zone into “excellent”, “very good”, and “good”, “moderate” and poor protective capacity zones. Areas classified into “moderate”, “very good” and “excellent” are more protected to contamination. The map of the study area mostly shows that the aquifer overburden protection capacity is “moderate” in the northeast portion of the study area with the longitudinal conductance values of 0 to 4 mhos and the portion of the map with longitudinal conductance values ranging from 5 mhos to 10 mhos classified as “very good” protective cover. The northwest portion of the map has an “excellent” protective capacity area with longitudinal conductance values ranging from 10 to 19 mhos and is a highly protected zone to contamination.

In the northwestern part of areas, the longitudinal conductance value is 0 to 1 mho classified as poor to moderate protective capacity. In the central part of the area, the unit longitudinal conductance varies from 0 to 1 mho and is distributed as a poor to moderate protective area.

In the south-eastern part of the area, the unit longitudinal conductance varies from 0 to 1 mho and is distributed as a poor to moderate protective area.

### 3.5. Physicochemical parameters

The hydrochemical analysis of water samples from different sites of District Bagh, Azad Jammu & Kashmir was also carried out.

The physico-chemical parameters of investigated water samples are shown in Table 3.

#### 3.5.1. pH

pH is the amount of concentration value hydrogen ion ( $H^+$ ) in water that demonstrates an acidic, basic or neutral solution. It regulates water corrosion and scaling tendency. pH high values in water are common scales while the pH low values indicate waters corrosive in nature. It also distresses aquatic life. Water with a pH of 7 is said to be neutral whereas lesser of it is stated acidic and the pH higher than 7 is considered as basic. Low pH water tends to be toxic and a high degree of pH water turned into an unpleasant taste [39].

The pH ranged from 6.98 to 7.67 (Table 3) with an average pH value of 7.302. The distribution of the water samples with respect to the pH (Fig. 15) values acquired are shown in Table 3. The standard range of pH for drinking water is 6.50–8.50, however, a value less than 6.50 is corrosive and a value above 8.50 showed the carbonated water (WHO and APHA Guidelines).

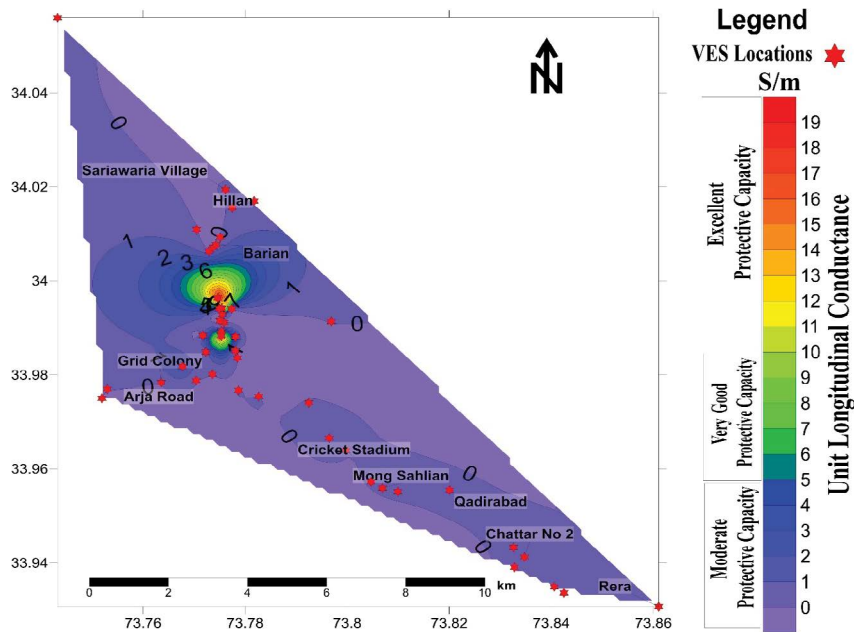


Fig. 14. Unit longitudinal conductance map of Bagh area.

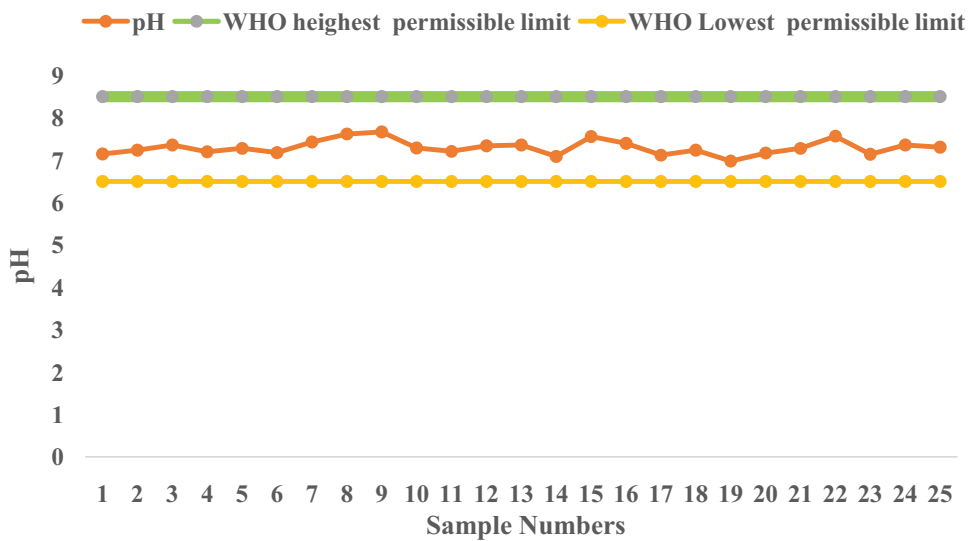


Fig. 15. pH results comparison with WHO guidelines.

In the southern part of the study area, the pH values indicated that sample number 1, sample number 4, sample number 6 and sample number 20 lie within the range of 7.14–7.21, while the sample number 19 area indicates the low ranged value of pH having value 6.98–7.06. The high values of pH in the study area are 7.6–7.67 indicated by sample number 8 and sample number 9.

The groundwater sample number 3, sample number 13, sample number 10, sample number 24 and sample number 25 in the northern and north-eastern part of the study area indicates the pH values 7.3–7.36 as shown in Table 3. These groundwater samples indicate the intermediate zone with respect to the values of pH in the study area.

### 3.5.2. Nitrate

Nitrate concentration was found in collected water samples ranging from BDL (below determinable limit) to 12.26 mg L<sup>-1</sup> (Fig. 16). Two water samples (sample number 9 and sample number 24) were observed to be above the APHA and WHO limits of 10.0 mg L<sup>-1</sup> for nitrate [40]. The nitrate concentration of ten samples is BDL (below the detection limit).

Nitrates (NO<sub>3</sub>) play a vigorous part in water contamination. Exceeding the nitrate (NO<sub>3</sub>) concentration contributes to the blood syndrome “Methemoglobinemia” which is commonly referred to as “Blue baby disorder” while the

Table 3  
The physico-chemical parameters of investigated water samples

S. No.	Colour	EC ( $\mu\text{S cm}^{-1}$ )	pH	Turb. (NTU)	Alk. ( $\text{mg L}^{-1}$ )	$\text{HCO}_3^-$ ( $\text{mg L}^{-1}$ )	Ca ( $\text{mg L}^{-1}$ )	$\text{CO}_3$ ( $\text{mg L}^{-1}$ )	Cl ( $\text{mg L}^{-1}$ )	Hard ( $\text{mg L}^{-1}$ )	Mg ( $\text{mg L}^{-1}$ )	K ( $\text{mg L}^{-1}$ )	Na ( $\text{mg L}^{-1}$ )	$\text{SO}_4$ ( $\text{mg L}^{-1}$ )	$\text{NO}_3$ ( $\text{mg L}^{-1}$ )	TDS ( $\text{mg L}^{-1}$ )
1	Colourless	558	7.15	BDL	242	242	61	BDL	12	282	32	1.8	9	14	2.82	307
2	Colourless	494	7.24	BDL	202	202	51	BDL	16	212	21	2.1	11	16	2.25	272
3	Colourless	463	7.36	BDL	252	252	49	BDL	14	252	32	1.7	8	14	1.38	255
4	Colourless	527	7.2	BDL	252	252	53	BDL	16	282	36	2	11	14	3.07	290
5	Colourless	469	7.28	BDL	202	202	41	BDL	12	242	34	1.6	10	17	2.26	258
6	Colourless	523	7.18	BDL	252	252	81	BDL	14	252	19	1.5	14	18	3.37	288
7	Colourless	405	7.43	BDL	182	182	17	BDL	14	202	39	1.7	8	14	1.36	223
8	Colourless	381	7.62	BDL	202	202	61	BDL	12	202	32	1.1	8	12	BDL	210
9	Colourless	983	7.67	BDL	402	402	69	BDL	60	562	70	5.7	18	25	12.26	590
10	Colourless	620	7.29	BDL	302	302	85	BDL	16	302	22	1.5	11	17	3.14	341
11	Colourless	888	7.21	BDL	402	402	61	BDL	26	412	63	3.5	16	20	5.85	488
12	Colourless	474	7.34	BDL	222	222	49	BDL	12	232	27	2.4	13	17	2.19	261
13	Colourless	380	7.36	BDL	182	182	41	BDL	20	202	24	1.4	7	13	BDL	209
14	Colourless	505	7.09	BDL	252	252	17	BDL	20	282	58	1.5	9	16	2.2	278
15	Colourless	336	7.56	BDL	182	182	17	BDL	12	192	36	1.1	7	12	BDL	185
16	Colourless	645	7.4	BDL	302	302	33	BDL	20	332	61	1	12	14	BDL	355
17	Colourless	463	7.12	3.59	252	252	61	BDL	14	252	24	0.9	4	10	BDL	255
18	Colourless	581	7.24	4.55	302	302	65	BDL	12	302	34	0.7	6	11	BDL	320
19	Colourless	683	6.98	1.24	302	302	65	BDL	38	352	46	0.9	18	18	BDL	376
20	Colourless	600	7.17	BDL	302	302	53	BDL	16	302	41	1.1	7	10	BDL	330
21	Colourless	401	7.28	BDL	202	202	41	BDL	12	232	32	1.3	8	15	BDL	221
22	Colourless	305	7.57	BDL	152	152	41	BDL	12	182	19	0.5	2	15	BDL	168
23	Colourless	502	7.14	BDL	252	252	47	BDL	12	302	45	1.9	11	26	2.87	276
24	Colourless	1985	7.36	BDL	372	372	121	BDL	390	552	61	1	210	57	11.08	1,191
25	Colourless	715	7.31	BDL	302	302	81	BDL	52	352	36	2.5	14	28	3.8	393
	WHO/APHA	NGVS	6.5–8.5	<5	NGVS	NGVS	NGVS	NGVS	250	500	NGVS	NGVS	NGVS	NGVS	10	1,000

WHO (World Health Organization)  
 APHA (American Public Health Association)  
 NGVS (No Guideline Value Set)  
 BDL (Below Detection Limit)

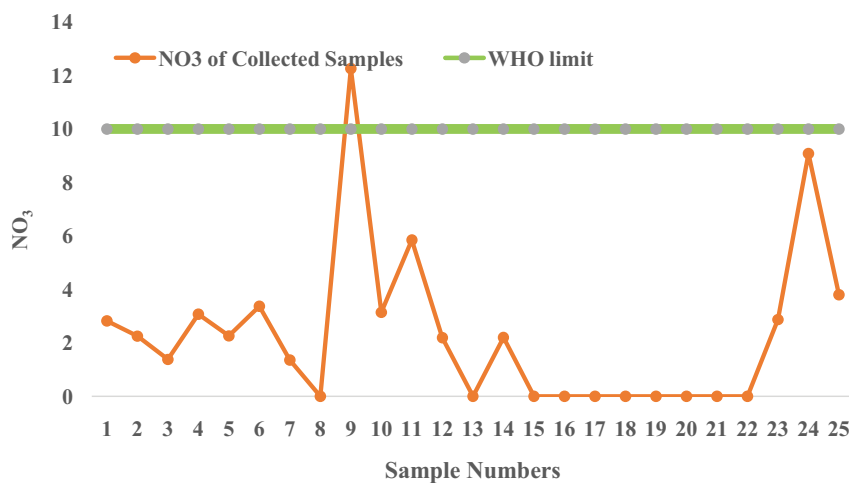


Fig. 16. Nitrate results comparison with WHO guidelines.

low concentration can cause muscle, tissue, and bones to work inadequately (WHO and APHA Guidelines). Table 3 shows the Nitrate concentration of groundwater samples in the project area.

Nitrate values present that sample number 3, sample number 7, sample number 8, sample number 13, sample number 15, sample number 16, sample number 18, sample number 19 and sample number 21 in the southern part of the study area lies in “low nitrate” zone with a range of 0–2.9 mg L<sup>-1</sup>.

The zone of sample number 9 (northeastern part of the study area) is considered as a high nitrate zone with nitrate values 10–12 mg L<sup>-1</sup> which is not suitable for drinking while the remaining other groundwater sample lies in the intermediate zone for nitrate.

### 3.5.3. Turbidity

The turbidity of collected water samples varied from 0 to 4.55 NTU and an average value of 0.375 NTU that is within the allowed limits of WHO and APHA (American Public Health Association) standards [41]. The turbidity values of 23 samples were BDL (below the determinable limit).

The variability turbidity presents that more than 75% of collected groundwater samples lie within a very low range or below the detection limit, these samples (sample number 1–16 and sample number 20–25) indicated a low turbidity zone. Sample number 19 areas show an intermediate zone for turbidity, while the zone of sample number 17 and sample number 18 (northeastern part of the study area) is relatively high for turbidity due to the presence of loose clay of the Murree Formation.

### 3.5.4. Hardness

Groundwater hardness is primarily due to the occurrence of the (Ca) and (Mg) divalent cations. It was resulting mostly from rock formations and the soil. Hard water generally, derives in regions where the topsoil is thick and calcareous formations are present [30].

The hardness of collected water samples ranges from 182.0 to 552.0 mg L<sup>-1</sup> (Fig. 17). The highest desirable limit is 500 mg L<sup>-1</sup>. One sample was observed to be above the WHO and APHA limits (500.0 mg L<sup>-1</sup>) for hardness.

Hardness values present in Table 3 Southern part of the study area sample number 2, sample number 7, sample number 8, sample number 13, sample number 15 and sample number 22 lie within the low hardness zone for the collected groundwater samples. These water samples represent the low hardness zone varies from 182 to 225 mg L<sup>-1</sup>. In the northern part of the study area, the sample number 24 is above the permeable limit for drinking water. Sample number 25 indicates an intermediate zone of hardness for the collected water samples.

### 3.5.5. Magnesium (Mg)

Mg is an important element for the human body and is very important for normal bone structure in the human body. Water with high magnesium or calcium levels is considered to be hard and is unwanted for drinking and household use [42].

In the research area, the Mg level for the collected samples ranged from 19.0 to 70.0 mg L<sup>-1</sup>.

The magnesium presents that sample number 2, sample number 6, sample number 13, sample number 17 and sample number 22 in the southern part of the study area lie within the low concentration area of magnesium for the collected groundwater samples, and having the values 19–25 mg L<sup>-1</sup>.

Sample number 19, sample number 4, sample number 20 in the southern part of the study area and sample number 25 in the northern part presents the intermediate zone of magnesium for the collected groundwater samples, while the remaining groundwater sample represents a higher concentration zone of magnesium for collected samples.

### 3.5.6. Calcium (Ca)

Calcium (Ca<sup>2+</sup>) high concentration may cause abdominal disorder and is problematic for drinking and domestic uses

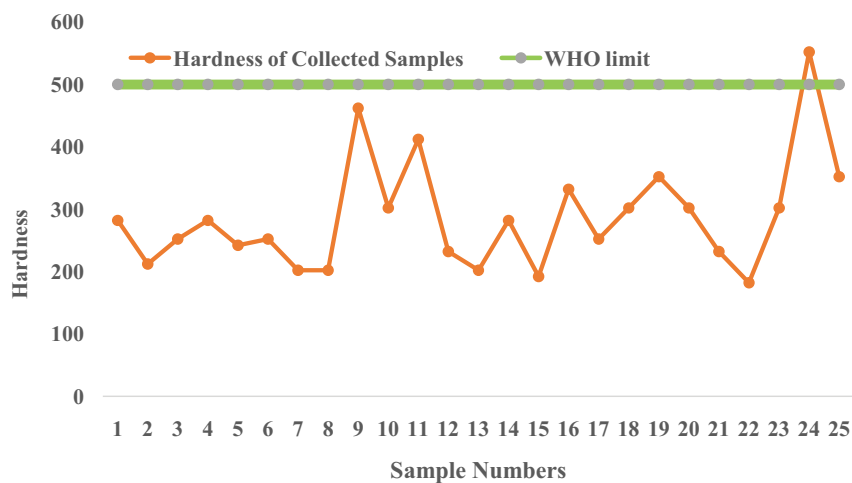


Fig. 17. Hardness results comparison with WHO guidelines.

as it leads to encrustation and scaling [43]. The occurrence of ( $\text{Ca}^{2+}$ ) in water supplies results from passageway above deposits of limestone, dolomite, gypsum, and Gypsi-ferrous shale.

In study area (Ca) concentration ranged 17.00 to 121.00  $\text{mg L}^{-1}$ . The average value of Ca is 54.44  $\text{mg L}^{-1}$ . Calcium (Ca) presents that sample number 7, sample number 14 and sample number 16 lie within the low concentration zone of calcium (Ca) having a range of 17–40  $\text{mg L}^{-1}$ .

Sample number 1, sample number 4, sample number 11, sample number 8, sample number 9, sample number 18, sample number 19, and sample number 20 in the southern part of the study area lies within the intermediate zone of calcium (Ca) for the collected groundwater samples.

### 3.5.7. Sodium (Na)

The role of sodium (Na) and chloride (Cl) in the human body is significant. Both elements influence the process of metabolism and physiologically. Large concentrations of sodium and chloride ions can cause high blood pressure.

The cation sodium (Na) of collected water samples ranged from 2.0 to 210.0  $\text{mg L}^{-1}$  with an average value of 18.08  $\text{mg L}^{-1}$ . All the samples were observed within the permissible limits.

Sodium (Na) presents sample number 1, sample number 2, sample number 3, sample number 4, sample number 5, sample number 6, sample number 7 and up to 21 in the southern part of the study area lies within the low concentration zone of sodium having the range of 2–25  $\text{mg L}^{-1}$ .

The only sample number 24 in the northern part lies within the high concentration zone of sodium for collected groundwater samples having a range of 187–208  $\text{mg L}^{-1}$  shown in Table 3.

### 3.5.8. Potassium (K)

Potassium is an incapable element for living organisms and essential for humans, plants, and animals. In the human body, the amount of potassium is 110.0–140.0 g. In the human body, potassium deficiency can disturb

heartbeat syndrome and muscle weakness, while homeostatic mechanisms may affect due to the high amount in potassium [44].

The cation potassium (K) of collected water samples ranged from 0.5 to 5.7  $\text{mg L}^{-1}$  with an average value of 1.696  $\text{mg L}^{-1}$ . The admissible limit of K is 12  $\text{mg L}^{-1}$  according to WHO guidelines. All the samples were observed within the allowable limits. Potassium (k) shows that sample number 16, sample number 17, sample number 18, sample number 19 and sample number 22 lie within the range of low potassium zone for the collected water samples and vary from 0.5 to 1.1  $\text{mg L}^{-1}$ .

Potassium (K) also shows that the only one collected groundwater from the north-eastern part of the study area (sample number 9) lies within the high potassium concentration zone having the value 5.2–5.7  $\text{mg L}^{-1}$  while remaining all the collected water samples shows the intermediate range of potassium as shown in Table 3.

### 3.5.9. Alkalinity

The alkalinity of groundwater is due to  $\text{HCO}_3^-$ ,  $\text{CO}_3^{2-}$  and hydroxide ions. In the research area, alkalinity ranged from 152.0 to 402.0  $\text{mg L}^{-1}$  [45]. All collected samples were found within the allowable limits of WHO guidelines. Alkalinity shows that sample number 2, sample number 5, sample number 7, sample number 8, sample number 13, sample number 15, sample number 21 and sample number 22 represent the low alkalinity zone for the collected groundwater samples.

The collected groundwater sample number 9 and sample number 10 from the eastern part of the study area indicated that the high alkalinity zone has a range of 375–402  $\text{mg L}^{-1}$ . Whereas the remaining water samples lie within the intermediate zone of the alkalinity having the range of 210–374  $\text{mg L}^{-1}$ .

### 3.5.10. Electrical conductivity

Electrical conductivity is the function of water's capability to pass electricity. Water conductivity is impaired by

the presence of inorganic dissolved solids, for example, Cl, NO<sub>3</sub>, SO<sub>4</sub>, and PO<sub>4</sub> anions (negatively charged) Na, Mg, Ca, Fe, and Al cations (positively charged ions) [46].

In the selected study area, EC ranges from 305.0 to 1985.0 with an average value of 595.44. Electrical conductivity shows that sample number 3, sample number 5, sample number 7, sample number 8, sample number 12, sample number 13, sample number 15, sample number 17, sample number 21 and sample number 22 represents the low electrical conductive zone for the collected groundwater samples, and having a range of 305–477.

Data shows only one collected sample (sample number 24) the northern part of the study area lies within the high electrical conductive zone having the value 1985, whereas the remaining samples of water show the intermediate level of electrical conductivity.

### 3.5.11. Sulphate, SO<sub>4</sub>

Sulphate (SO<sub>4</sub>) is a product of sulphur (S) and oxygen (O) and is part of naturally occurring minerals in certain soil and rock formations bearing groundwater [46]. Over time the mineral dissolves and is discharged into groundwater, as water moves into soil and rock formations containing sulphate minerals. SO<sub>4</sub> is released into the aquatic environment in wastes from industries that use SO<sub>4</sub> and H<sub>2</sub>SO<sub>4</sub>, such as mining and casting processes, paper industry and tanneries [32]. World Health Organization has set the maximum level of sulphate contaminants in drinking water at 250 mg L<sup>-1</sup>.

Sulphates (SO<sub>4</sub>) value varies from 10.0 ppm to 57.0 ppm with an average value of is sulphates (SO<sub>4</sub>) 17.72 ppm. Sulphate (SO<sub>4</sub>) salts in water may rise the corrosion of mild steel in the delivery system.

Table 3 shows that sample number 1, sample number 3, sample number 4, sample number 7, sample number 8, sample number 15, sample number 16, sample number 17, sample number 18 and sample number 21 from the southern part of the study area indicates the low sulphate zone for the water samples and varies from 10–15 mg L<sup>-1</sup>. Data presents that only one collected water sample (sample number 24)

from the northern part of the area shows a high concentration zone of sulphate while other water samples show an intermediate level of sulphate.

### 3.5.12. Chloride (Cl)

Chloride in groundwater and surface water may occur naturally in deep aquifers, due to contamination from marine, household or industrial wastes. Chloride (Cl) is extensively disseminated in nature as sodium, potassium and calcium salts. The maximum limit for chloride is 250 ppm.

The chlorides (Cl) value varies from 12.0 to 390 ppm with an average value of 34.16 ppm (Fig. 18). One water sample was observed to be exceeding the limits of the World Health Organization and APHA (250.0 mg L<sup>-1</sup>). Chloride (Cl) raises the water’s electrical conductivity and therefore increases its corrosion. Table 3 shows that sample numbers 1 to 8 and sample numbers 12 up to 23 from the southern part of the area indicated that a low chloride concentration with the range of 12–54 mg L<sup>-1</sup>.

Data shows only one water sample (sample number 24) northern part of the study area high concentration of chloride in the research area with a value of 390 mg L<sup>-1</sup>, whereas the other water samples show the intermediate level of chloride.

### 3.5.13. Total dissolved solids

The TDS values of the water samples varied from 168 to 1,191 mg L<sup>-1</sup> with an average of 336.6 mg L<sup>-1</sup> (Fig. 19). The WHO guiding principle permits a maximum level of 1,000 mg L<sup>-1</sup>. One water sample was observed to be higher than the WHO (World Health Organization) and APHA guidelines (1,000 mg L<sup>-1</sup>).

The level of total dissolved solids also reflects the level of salinity of the water, for example, total dissolved solids less than 200 mg L<sup>-1</sup> is low salinity; TDS 200–500 mg L<sup>-1</sup> average salinity; TDS 500–1,500 mg L<sup>-1</sup> high salinity and total dissolved solids greater than 1,500 mg L<sup>-1</sup> very high salinity. The calculated values of TDS show that only one collected sample reduced the groundwater quality and pose a major health risk. TDS present that the sample number 2, sample

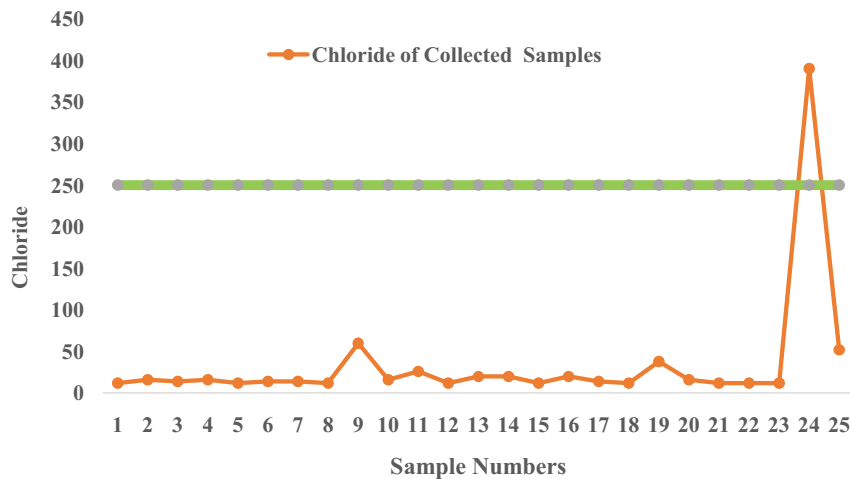


Fig. 18. Chloride results comparison with WHO guidelines.

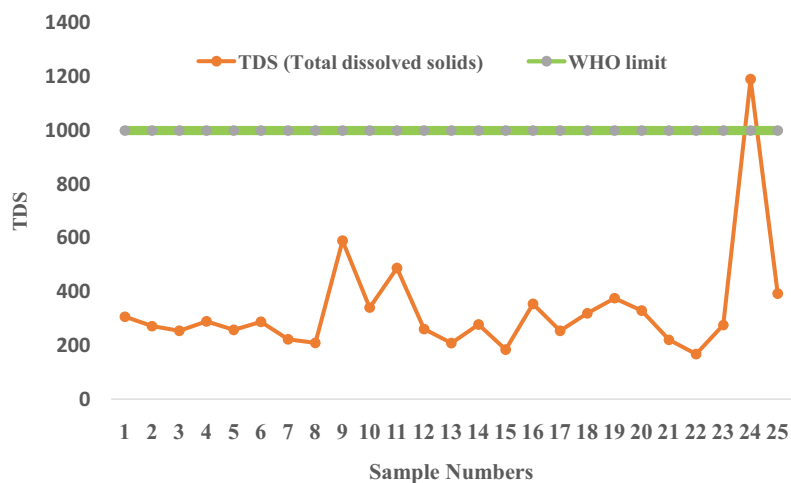


Fig. 19. TDS results comparison with WHO guidelines.

number 5, sample number 7, sample number 8, sample number 12, sample number 13, sample number 14, sample number 15, sample 17, sample number 21 and sample number 22 from the southern part of the area shows the low level of dissolved solids within the research area and varies from 168–284 mg L<sup>-1</sup> while the map shows only one water sample indicates the high level of TDS within the research area.

#### 3.5.14. Carbonates (CO<sub>3</sub>)

Carbonates (CO<sub>3</sub>) values of all collected water samples were BDL (below detection limit).

#### 3.5.15. Bicarbonates (HCO<sub>3</sub>)

In collected water samples the concentration of bicarbonates varies from 152.0 to 402.0 mg L<sup>-1</sup> with an average value of 258.8 mg L<sup>-1</sup>. Bicarbonates (HCO<sub>3</sub>) values recommended by WHO are not more than 500 mg L<sup>-1</sup>.

The existence of HCO<sub>3</sub> in the water suggested, either weathering of silicate or weathering of carbonate and occasionally it may be due to both processes [32]. Mostly, whenever carbonic acid reacts with calcium carbonate, bicarbonate is released together with calcium. Similarly, if carbonic acid reaction with plagioclase, bicarbonate can be released. It is also commonly found in my water samples and in some industrial wastes [33]. Bicarbonate shows that the three water samples (sample number 9, sample number 11 and sample number 24) from the north and eastern part of the study area indicated a high concentration zone of bicarbonates for collected water samples and having a range of 375–402 mg L<sup>-1</sup>, whereas the only one water sample (sample number 22) the northern part of the area shows that low concentration values for bicarbonates. Whereas remaining water samples lie within the intermediate range of bicarbonates.

The piper diagram for the chemical parameters of the water sample has been plotted [46]. The results in Fig. 20 show that all the samples belong to type 1 (Ca–HCO<sub>3</sub>). Furthermore, it is also the indication of excess of alkaline earth metals (Ca + Mg) than the alkalis (Na + K) resulting from the dissolution of Ca–Mg dominant rocks.

#### 3.6. Integration between VES and hydrochemical analysis

The vulnerability mapping using geoelectrical data demarcated different moderate to high overburden protective capacity zones in the study area. Geoelectrical data also confirmed that there is no area with “very low protective overburden capacity”. Similarly, hydrochemical analysis results indicate that twenty-three springs and wells are suitable for drinking purposes, except where exceed the permissible limit of total hardness, Chlorides and Nitrate. The contamination in the two samples (sample number 9 and sample number 24) northeastern part of the study area was detected from the area of “moderate overburden protective capacity” in the vulnerability map. The top layers at these locations were deposits sand gravel and clay. The integrated study results delineated that the vulnerability mapping from the geophysical survey is authentic, low-cost and useful as compared to costly laboratory analysis.

#### 4. Conclusion

The present research has proven that integration between VES and hydrochemical analysis provides a reliable insight into the local groundwater systems in terms of quality and occurrence of saturated zones. A total of 45 VES points acquired in different parts of the area represented the majority of subsurface lithologies, landform geomorphic features of the area. The VES inversion results depicted 4 layers having aquifer body in the 2nd and 3rd layers. The overall depth of the VES data ranges between 50–100 m. the major lithologies identified by VES data comprise of clay, sandy clay, clay with boulder, and sandstone. The iso-resistivity maps generated at variable depths depicted the good water quality in the north-west and south-eastern part of the area. The aquifer thickness map indicated the maximum thickness of 60 m at a spread in the south west to the north-eastern part. The large thickness of the aquifer suggests a large subsurface zone that can transmit economical quantities of water for local community and industry. Overall groundwater production is approximated as a medium to high for the area. The unit longitudinal map indicated

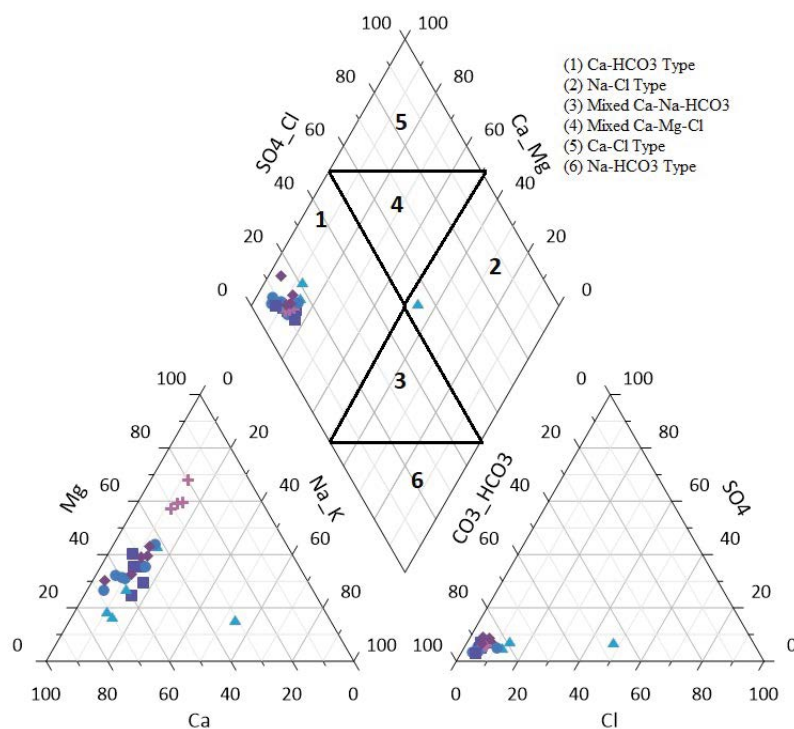


Fig. 20. Piper diagram of water samples.

values ranging between 0–19 mhos. These values suggest moderate to good protective capacity in the majority part of the area. Poor to moderate capacity is only seen in parts of the north and east. These are the locations where hydrochemical samples also depicted poor groundwater quality.

The hydrochemical analysis results indicate that out of 24, 22 samples lie within the permissible ranges of WHO. The 2 samples which were not within permissible limits were acquired. The integration between VES and hydrochemical analysis also provided a strong correlation between the findings as samples that were not in the permissible limits (sample number 9 and sample number 24) were detected from the area of “moderate over-burden protective capacity” in the vulnerability map. The integrated study results delineated that the vulnerability mapping from the geophysical survey is authentic, low-cost and useful as compared to costly laboratory analysis.

#### Acknowledgment

The authors are thankful to the Director Institute of Geology UAJ&K Muzaffarabad for financial assistance to carry out fieldwork and lab analysis work.

#### References

- [1] D.R. Rahmawati, Supriyadi, N.P. Aryani, M.A. Naufal, Groundwater potential prediction by using geoelectricity method a case study in Simpang Lima and around it, *J. Phys. Conf. Ser.*, 983 (2018) 012003, doi: 10.1088/1742-6596/983/1/012003.
- [2] S.P. Gorde, M.V. Jadhav, Assessment of water quality parameters. A review, *Int. J. Eng. Appl. Sci.*, 3 (2013) 2029–2035.
- [3] T. Ahmed, A. Pervez, M. Mehtab, S.K. Sherwani, Assessment of drinking water quality and its potential health impacts in academic institutions of Abbottabad Pakistan, *Desal. Water Treat.*, 7 (2014) 1819–1828.
- [4] A. Niaz, M. Imtiaz, M.R. Khan, F. Hameed, J. Niaz, A.Y. Khan, K. Mehmood, The use of GIS and geo-electric techniques for delineation surface and groundwater potential in Kotli City, District Kotli, Azad Jammu and Kashmir, Pakistan, *Pak. J. Eng. Appl. Sci.*, 26 (2020) 1–15.
- [5] S. Gaikwad, N.J. Pawar, P. Bedse, V. Wagh, A. Kadam, Delineation of groundwater potential zones using vertical electrical sounding (VES) in a complex bedrock geological setting of the West Coast of India, *Model. Earth Syst. Environ.*, (2021), doi: 10.1007/s40808-021-01223-3.
- [6] A. Niaz, R.M. Khan, U. Ijaz, M.Y. Khan, F. Hameed, Determination of groundwater potential by using geoelectrical method and petrographic analysis in Rawalakot and adjacent areas of Azad Kashmir, sub-Himalayas, Pakistan, *Arabian J. Geosci.*, 11 (2017) 55, doi: 10.1007/s12517-018-3811-0.
- [7] A. Stampolidis, P. Tsourlos, P. Soupios, T.H. Mimides, G. Tsokas, G. Vargemezis, A. Vafidis, Integrated geophysical investigation around the brackish spring of Rina, Kalimnos Island Greece, *Balk Geophys. Soc.*, 8 (2005) 63–73.
- [8] P. Soupios, M. Kouli, F. Vallianatos, A. Vafidis, G. Stavroulakis, Estimation of aquifer parameters from surficial geophysical methods. A case study of Keritis Basin in Crete, *J. Hydrol.*, 338 (2007) 122–131.
- [9] D. Kalisperi, P. Soupios, M. Kouli, P. Barsukov, S. Kershaw, P. Collins, F. Vallianatos, Coastal Aquifer Assessment Using Geophysical Methods (TEM, VES), Case Study: Northern Crete, Greece, 3rd IASME/WSEAS International Conference on Geology and Seismology (GES '09) Cambridge, UK, 2009, pp. 24–26.
- [10] V. Kadam, S. Wagh, B. Patil, R. Umrikar, R. Sankhua, Seasonal assessment of groundwater contamination, health risk and chemometric investigation for a hard rock terrain of western India, *Environ. Earth Sci.*, 80 (2021) 172, doi: 10.1007/s12665-021-09414-y.

- [11] B. Redhaouia, M. Bédir, H. Gabtni, O.I. Batobo, M. Dhaoui, A. Chabaane, S. Khomsi, Hydro-geophysical characterization for groundwater resources potential of fractured limestone reservoirs in Amdoun Monts (North-western Tunisia), *J. Appl. Geophys.*, 128 (2016) 150–162.
- [12] V. Kadam, J. Wagh, S. Jacobs, N. Patil, B. Pawar, R. Umrikar, S. Sankhua, S. Kumar, Integrated approach for the evaluation of groundwater quality through hydro geochemistry and human health risk from Shivganga river basin, Pune, Maharashtra, India, *Environ. Sci. Pollut. Res.*, 29 (2022) 4311–4333.
- [13] M. Bersi, H. Saibi, Groundwater potential zones identification using geoelectrical sounding and remote sensing in Wadi Touil plain, Northwestern Algeria, *J. Afr. Earth Sci.*, 172 (2020) 104014, doi: 10.1016/j.jafrearsci.2020.104014.
- [14] F. Bahri, H. Saibi, Characterization, classification, and determination of drinkability of some Algerian thermal waters, *Arabian J. Geosci.*, 4 (2011) 207–219.
- [15] H. Saibi, F. Bahri A. Semar, Hydrochemistry and bacteriology of western and Saharan spring waters of Algeria, *Arabian J. Geosci.*, 6 (2013) 665–677.
- [16] J.E. Liggett, S. Talwar, Groundwater vulnerability assessments and integrated water resource management, *Watershed Manage. Bull.*, 13 (2009) 18–29.
- [17] V.M. Wagh, D.B. Panaskar, J.A. Jacobs, S.V. Mukate, A.A. Muley, A.K. Kadam, Influence of hydro-geochemical processes on groundwater quality through geostatistical techniques in Kadava River basin, Western India, *Arabian J. Geosci.*, 12 (2019) 1–25, doi: 10.1007/s12517-018-4136-8.
- [18] Z.A. Soomro, M.A. Khokhar, W. Hussain, M. Hussain, Drinking Water Quality Challenges in Pakistan, Pakistan Council of Research in Water Resources, Lahore, 2011, pp. 17–28.
- [19] S.M.I. Shah, Stratigraphy of Pakistan, Memoir of Geological Survey of Pakistan, 2009.
- [20] S.S. Asadi, P. Vuppala, M.A. Reddy, Remote sensing and GIS techniques for evaluation of groundwater quality in Municipal Corporation of Hyderabad (Zone-V), India, *Int. J. Environ. Res. Public Health*, 4 (2007) 45–52.
- [21] B.A. Skubon, Groundwater Quality and GIS Investigation of a Shallow Sand Aquifer, Oak Opening Region, Geolog. Soc. America Abstracts Programs, North West Ohio, 2005.
- [22] S. Yammani, Groundwater quality suitable zones identification: application of GIS, Chittoor area, Andhra Pradesh, India, *Environ. Geol.*, 53 (2007) 201–210.
- [23] A. Niaz, M.R. Khan, S. Mustafa, F. Hameed, Determination of aquifer properties and vulnerability mapping by using geoelectrical investigation of parts of Sub-Himalayas, Bhimber, Azad Jammu and Kashmir, Pakistan, *Q. J. Eng. Geol. Hydrogeol.*, 49 (2016) 36–46.
- [24] A. Sarangi, C.A. Madramootoo, P. Enright, Comparison of spatial variability techniques for runoff estimation from a Canadian watershed, *Biosyst. Eng.*, 95 (2006) 295–308.
- [25] B.U. Nisar, M.R. Khan, S. Khan, M. Farooq, M. Rizwan, K.A. Ahmed, S.S. Razzaq, A. Niaz, Quaternary Paleodepositional Environments in relation to Ground water occurrence in lesser Himalayan Region, Pak. *J. Himalayan Earth Sci.*, 51 (2018) 99–112.
- [26] A. Niaz, M.R. Khan, A. Asghar, S. Mustafa, F. Hameed, B.N. Umair, S. Khan, M.S. Mughal, M. Farooq, M. Rizwan, The study of aquifers potential and contamination based on geoelectric technique and chemical analysis in Mirpur Azad Jammu and Kashmir, Pak. *J. Himalayan Earth Sci.*, 50 (2017) 60–73.
- [27] E.O. Joshua, O.O. Odeyemi, O.O. Fawehinmi, Geoelectric investigation of the groundwater potential of Moniya Area, Ibadan, *J. Geol. Min. Res.*, 3 (2011) 54–62.
- [28] S.K. Pal, R.K. Majumdar, Determination for groundwater potential zones using iso-resistivity map in the alluvial areas of Munger District, Bihar, *J. Earth Sci.*, 1 (2001) 16–26.
- [29] A. Zohdy, V. Eaton, D. Mabey, Application of surface geophysics to groundwater investigations. *Techniques of Water-Resources Investigation*, US Geol. Surv., 2 (1974) 116–119.
- [30] D.S. Parasnis, *Principle of Applied Geophysics*, 3rd ed., Chapman and Hall, London, 1979, p. 275.
- [31] E. Martinelli, Groundwater exploration by geoelectrical methods in Southern Africa, *Bull. Eng. Geol.*, 15 (1978) 113–124.
- [32] J. Oseji, M. Asokhia, E. Okolie, Determination of groundwater potential in obiaruku and environs using surface geoelectric sounding, *Environmentalist*, 26 (2006) 301–308.
- [33] M.H. Khalil, Hydro-geophysical configuration for the quaternary aquifer of Nuweiba alluvial fan, *J. Eng. Geophys.*, 15 (2010) 77–90.
- [34] P. Sikandar, A. Bakhsh, M. Arshad, T. Rana, The use of vertical electrical sounding resistivity method for the location of low salinity groundwater for irrigation in Chaj and Rachna Doabs, *Environ. Earth Sci.*, 60 (2010) 1113–1129.
- [35] J.P. Henriot, Direct application of the Dar Zarrouk parameters in groundwater surveys, *Geophys. Prospect.*, 24 (1976) 344–353.
- [36] C. Nwanko, L. Nwasu, G. Emujakporue, Determination of Dar Zarouk parameters for assessment of groundwater potential: case study of Imo State, south eastern Nigeria, *J. Econ. Sustain. Dev.*, 2 (2011) 571.
- [37] L. Slater, Near-surface electrical characterization of hydraulic conductivity from petro physical properties to aquifer geometries, *Revised Surv. Geophys.*, 28 (2007) 167–169.
- [38] K. Arumugam, Assessment of Groundwater Quality in Tirupur Region, Ph.D. Thesis (Unpublished), Anna University, Chennai, 2010.
- [39] S.K. Kumar, A. Logeshkumaran, N.S. Magesh, P.S. Godson, N. Chandrasekar, Hydro-geochemistry and application of water quality index (WQI) for groundwater quality assessment, Anna Nagar, part of Chennai City, Tamil Nadu, India, *Appl. Water Sci.*, 5 (2015) 335–343.
- [40] C.E. Delisle, J.W. Schmidt, The Effects of Sulphur on Water and Aquatic Life in Canada, In: Sulphur and its Inorganic Derivatives in the Canadian Environment, NRCC No. 15015, Associate Committee on Sci. Criteria for Environ. Quality, National Research Council of Canada, Ottawa, 1977.
- [41] L. Elango, R. Kannan, Rock–water interaction and its control on the chemical composition of groundwater, *Dev. Environ. Sci.*, 5 (2007) 229–243.
- [42] U.B. Nisar, M.J. Khan, M. Imran, M.R. Khan, M. Farooq, S.A. Ehsan, A. Ahmad, H.H. Qazi, N. Rashid, T. Manzoor, Groundwater investigations in the Hattar industrial estate and its vicinity, Haripur district, Pakistan: an integrated approach, *Kuwait J. Sci.*, 48 (2021) 1, doi: 10.48129/kjs.v48i1.7820.
- [43] H. Saibi, M. Mesbah, A.S. Moulla, A. Guendouz, S. Ehara, Principal component, chemical, bacteriological, and isotopic analyses of Oued-Souf groundwaters (Revised), *Environ. Earth Sci.*, 75 (2016) 1–17.
- [44] M. Djemai, H. Saibi, M. Mesbah, A. Robertson, Spatio-temporal evolution of the physico-chemical water characteristics of the Sebaou river valley (Great Kabylia, Algeria), *J. Hydrol. Region Stud.*, 12 (2017) 33–49.
- [45] F. Bahri, H. Saibi, Characterization, classification, bacteriological, and evaluation of groundwater from 24 wells in 6 departments of Algeria, *Arabian J. Geosci.*, 5 (2012) 1449–1458.
- [46] N. Darwesh, M. Allam, Q. Meng, A. Helfdhallah, N.S.M. Ramzy, K. Kharrim, A.A. Al Maliki, D. Belghyti, Using Piper trilinear diagrams and principal component analysis to determine variation in hydrochemical faces and understand the evolution of groundwater in Sidi Slimane Region, Morocco, Egypt. *J. Aquat. Biol. Fish.*, 23 (2019) 17–30.